Progress In Electromagnetics Research C, Vol. 111, 119–133, 2021

On the Performance of Reconfigurable Intelligent Surface Aided Power Line Communication System under Different Relay Transmission Protocols

Kehinde O. Odeyemi[1, 2, *], Pius A. Owolawi[1], and Oladayo O. Olakanmi[2]

Abstract—In this paper, the performance analysis of a dual-hop reconfigurable intelligent surface (RIS)-aided power line communication (PLC) system is presented under different relay transmission protocols. The relay is assumed to be decode-and-forward (DF) or amplify-and-forward (AF) relaying protocol. It is also assumed that the RIS link is subjected to Rayleigh fading while the PLC link undergoes Log-normal fading with the influence of additive background and impulsive noise. To evaluate the system performance, the end-to-end cumulative distribution function for both relaying protocols are derived. Based on these, the analysis expressions for the system outage probability and average bit error rate (ABER) are derived under DF and AF relaying protocols. To gain further insight about the system performance, the asymptotic analysis for the derived expressions is obtained at high signal-to-noise ratio regime. The findings illustrate the significant impact of the number of RIS elements and impulsive noise on the overall system performance. In addition, the accuracy of the analytical results is justified through Monte-Carlo simulations.

1. INTRODUCTION. BACKGROUND INFORMATION

In recent time, power line communication (PLC) systems have been considered as a competitive technology for high-speed data transmission through the utilization of existing and pre-installed power line networks for the distribution of both information and power [1]. The system has significant advantages of providing last mile access to end users and reduces the cost of deployment. As a result of this, it has been considered as a feasible candidate for indoor and outdoor applications such as home-networking, control applications, and smart metering [2]. However, with all these excellent features, the PLC system is highly susceptible to various channel impairments which degrade the link reliability. Specifically, the PLC link generates electromagnetic interference which affects the surrounding wireless systems [3]. In addition, PLC link suffers from two types of noises, i.e., impulsive noise and background noise which results in data loss. The impulse noise is a random occurring noise with high power spectral density (PSD) and short duration. The background noise is negligible over time with low PSD [4]. Owing to frequency selectivity, the link also suffers from attenuation which can deteriorate the system achievable data rate and also introduces inter-symbol interference. This becomes more pronounced at high frequencies and with the increase in distance between the transmitter and receiver [3, 5, 6].

Today, reconfigurable intelligent surface has gain considerable attention in the research community owing to its applications in the next-generation wireless communication systems [7]. Compared with other technologies counterparts, it requires no complex encoding and decoding without additional power supply for signal transmission [8, 9]. They can be easily deployed on different infrastructural

Received 8 February 2021, Accepted 17 March 2021, Scheduled 26 March 2021
* Corresponding author: Kehinde O. Odeyemi (kesonics@yahoo.com).
[1] Department of Computer Systems Engineering, Tshwane University of Technology, Pretoria-0001, South Africa. [2] Department of Electrical and Electronic Engineering, Faculty of Technology, University of Ibadan, Nigeria.

surfaces such walls, ceilings, and buildings in order to reflect the transmitted signal [10]. Thus, as a new innovation technology, it employs a large number of low-cost passive elements which have the capacity of intelligently controlling the characteristics of the receive signals such as amplitude phase and polarisation [11, 12]. As a result of this, it eliminates the obstruction effects and improves the system spectral and energy efficiency compared to conventional diversity systems. The increase in the number of reflecting elements in RIS significantly enhances the quality of the received signal [13].

Over the time, relay-assisted technology has been considered as a promising technology to improve the reliability and coverage of wireless communication systems against fading effects. This can be achieved using two types of relaying protocols, i.e., amplify-and-forward (AF) and decode-and-forward relaying protocols. The former amplifies the received signal and resend it to the destination while the latter decodes and re-encodes the received signal before transmitting to the destination [1]. Based on this, relay-assisted PLC systems have been widely studied in open literature. In [14], the performance of an RF-assisted PLC system over Log-normal distribution with Bernoulli-Gaussian impulsive noise was studied. Also, the performance of a half-duplex PLC system was evaluated in [15] under AF and DF relaying protocols. The authors in [16] investigated the performance of a full-duplex AF relaying PLC system with the derivation of outage probability, average error rate, and average capacity performance metrics. Moreover, the physical layer security of the PLC relay-aided system was presented in [17] under the eavesdropper and noise interference. Recently, the performance of a dual-hop PLC/RF system was studied in [4] under the AF and DF relaying scheme. The authors obtained analytical closed-form expressions in terms of outage probability, average error rate, and average capacity. However, in all these aforementioned works, RIS was not considered for the signal transmission to the system destination. To the best of the authors' knowledge, the study of RIS as a relay aided technique for wireless communication systems is still at infancy stage. In [18], the performance of a dual-hop RIS-assisted free space optical (FSO)/RF system was investigated. Also, the authors in [19] considered RIS in the FSO setup to increase the system coverage and performance. The performance of a dual-hop unmanned aerial vehicle communication was studied in [20] where RIS was used to improve the system performance and coverage area. Moreover, the performance of a DF dual-hop RIS-assisted underwater optical communication system was evaluated in [8] where the system outage probability and average error rate were derived. In all these stated works, it can be observed that the systems are not PLC-based systems.

Motivated by the above facts, the performance of a dual-hop relay assisted PLC system under DF and AF relaying protocols is presented. The PLC link is assumed to follow the Log-normal distribution with the effect of additive background and impulsive noise while the RIS link is subjected to Rayleigh distribution. The equivalent CDF for the concerned system under both DF and AF is derived. By utilizing the derived CDF, the concerned system outage probability and average error rate are obtained. To further gain more insight about the derived expressions, the asymptotic expressions at high signal-to-noise ratio (SNR) are determined. Thus, the main contributions in this study are stated as follows:

(i) The equivalent end-to-end CDF for the concerned system is derived for both DF and AF relaying protocols.

(ii) The system analytical closed-form expressions for the outage probability and ABER are derived for both relaying protocols.

(iii) The asymptotic expressions for the system outage probability and ABER are determined at high SNR.

The remainder of this paper is structured as follows. Section 2 illustrates the system and channel models. In Section 3, the statistical end-to-end analysis of each link is provided. The performance analysis of the system with asymptotic analysis is detailed in Section 4. In Section 5, the numerical results with discussions are presented. Finally, Section 6 gives the paper's conclusion remarks.

2. SYSTEM AND CHANNEL MODELS

As illustrated in Figure 1, a dual-hop RF-RIS assisted PLC system is presented, where the source (S) communicates with the destination (D) via the relay (R) and RIS. The RIS consists of N number of reflecting elements with full knowledge of channel state information while the S, R, and D are equipped

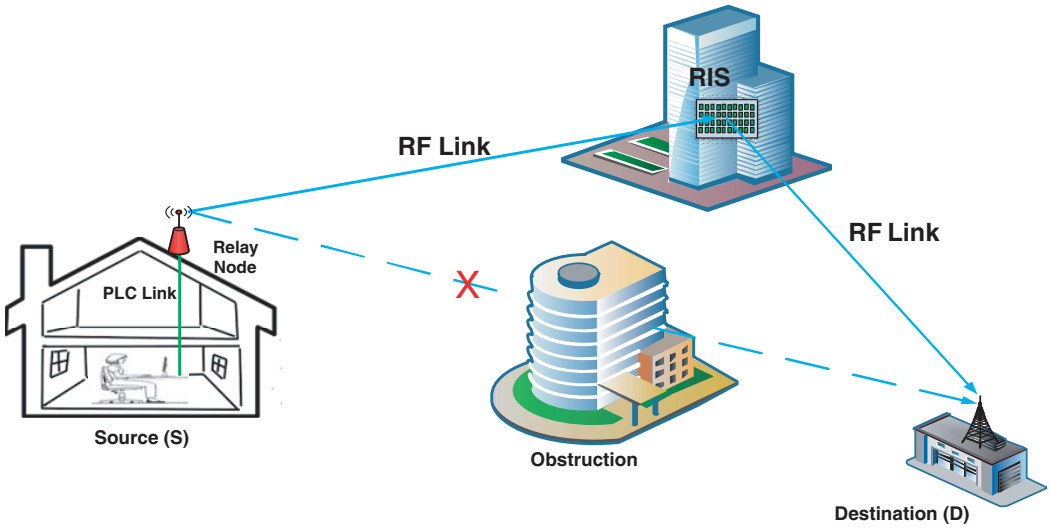

Figure 1. A dual-hop RF-RIS aided PLC system model.

with a single antenna. Also, it is assumed that there is no direct link between the relay and the destination owning to buildings obstruction, and communication is performed through the RIS forming an intelligent environment for the signal quality improvement. Similar to cooperative-based systems, the concerned system operates in half duplex mode, and entire information transmission occurs in two time slots.

During the first time slot, the source sends its message to the relay node via the PLC link using binary modulation scheme. Thus, the signal received at the relay node can be expressed as:

$$y_R^{PLC} = h_{PLC}s + Z_{PLC} \tag{1}$$

where h_{PLC} is the channel fading gain of the PLC link, s the source message, and Z_{PLC} the additive noises present in the PLC link. Owing to many switching transients and low-power noise sources along the PLC link, the link is highly prone to the effect of additive background noise and impulsive noise. Statistically, the study of both noise effects on the PLC link can be modeled by using a Poisson-Gaussian mixture model given as [21]:

$$Z_{PLC} = n_i + n_b \tag{2}$$

where $n_i = i_p i_I$ with i_p denotes the arrival of the impulsive noise which follows Poisson process, and i_I signifies the additive white Gaussian noise (AWGN) with zero mean and variance σ_I^2. n_b represents the background noise that follows AWGN with zero mean and variance σ_B^2. By considering only the background noise samples on the PLC link, the link instantaneous SNR can be defined as [22]:

$$\gamma_{PLC1} = \frac{E_b \left|h_{PLC}\right|^2}{\sigma_B^2} = \bar{\gamma}_{PLC1} \left|h_{PLC}\right|^2 \tag{3}$$

where E_b is the average signal energy, and $\bar{\gamma}_{PLC1}$ denotes the average link SNR when background noise samples occur on the link. When both the background noise and impulsive noise samples occur on the PLC link, the link instantaneous SNR can be given as [21]:

$$\gamma_{PLC2} = \frac{E_b \left|h_{PLC}\right|^2}{\sigma_B^2 \left(1+\xi\right)} = \bar{\gamma}_{PLC2} \left|h_{PLC}\right|^2 \tag{4}$$

where $\xi = \sigma_I^2/\sigma_B^2$ is the impulse ratio parameter which signifies the ratio of impulsive noise power to background noise power, and $\bar{\gamma}_{PLC2}$ denotes the average link SNR when both noises occur on the link

During the second time slot, the relay transmits the received source message to the destination via the RIS. In the case of DF relaying protocol, the received signal at the destination can then be expressed

as:

$$y_D^{RIS,\,DF} = \sum_{n=1}^{N} h_n v_n \exp\left(j\phi_n\right)\hat{s} + Z_D \tag{5}$$

where ϕ_n denotes the adjustable phase induced by the n-th reflector elements, $\hat{s}$ the source information transmitted by the RIS, and Z_D the AWGN at the destination with zero mean and σ_D^2 variance. Also, $h_n = w_n \exp(-j\theta_n)$ and $v_n = b_n \exp(-j\psi_n)$ are the channel gains of the R-to-RIS and RIS-to-D links, respectively with ν_i and u_i respectively the amplitudes of the Rayleigh distribution, and θ_n and ψ_n are the phases. In order to eliminate the channel phase, $\phi_n = \theta_n + \psi_n$ so as to maximise the SNR at the destination. Thus, the instantaneous SNR at the destination can then be expressed as [8]:

$$\gamma_D = \bar{\gamma}_{RIS} \left(\sum_{n=1}^{N} w_n b_n \right)^2 = \bar{\gamma}_{RIS} R^2 \tag{6}$$

where $\bar{\gamma}_{RIS}$ represents the average SNR at the destination

Under the AF relaying protocol, the received signal at the destination can be written as:

$$y_D^{RIS,AF} = \sum_{n=1}^{N} h_n v_n \exp\left(j\phi_n\right) G y_R^{PLC} + Z_D \tag{7}$$

where G denotes the fixed gain.

2.1. PLC Link Model

The PLC link suffers from the fading effect owing to mismatching of impedance and multipath fading along the link. As a result of this, the link is generally assumed to follow the Log-normal fading distribution. Therefore, for analysis simplification and to achieve a traceable closed-form expression, the PLC link probability distribution function (PDF) of the SNR γ_{PLC} is given by approximating Log-normal PDF with Gamma PDF as [4, 22]:

$$f_{\gamma_{PLC}}(\gamma) = (1 - P_s) \left(\frac{m_1}{\Omega_1}\right)^{m_1} \frac{\gamma^{m_1 - 1}}{\Gamma(m_1)} \exp\left(-\frac{m_1}{\Omega_1}\gamma\right) + P_s \left(\frac{m_2}{\Omega_2}\right)^{m_2} \frac{\gamma^{m_2 - 1}}{\Gamma(m_2)} \exp\left(-\frac{m_2}{\Omega_2}\gamma\right) \tag{8}$$

where $P_s = \lambda_s T_s$ is the probability of occurrence of the impulsive noise in the PLC link with λ_s and T_s respectively denoting the arrive rate and duration of occurrence of impulse noise, and m_1 and m_2 are the link shadowing severity parameters of the Gamma PDF. Ω_1 and Ω_2 signify the link mean power of the Gamma PDF, and $\Gamma(\cdot)$ denotes the Gamma function.

Thus, the PLC link cumulative distribution function (CDF) of the SNR γ_{PLC} can be obtained by integrating Eq. (8) using the integration identity given in [23, Eq. (8.4.16)] as:

$$F_{\gamma_{PLC}}(\gamma) = \frac{(1 - P_s)}{\Gamma(m_1)} G_{1,2}^{1,1}\left(\frac{m_1}{\Omega_1}\gamma \middle| \begin{matrix} 1 \\ m_1,\, 0 \end{matrix}\right) + \frac{P_s}{\Gamma(m_2)} G_{1,2}^{1,1}\left(\frac{m_2}{\Omega_2}\gamma \middle| \begin{matrix} 1 \\ m_2,\, 0 \end{matrix}\right) \tag{9}$$

where $G_{p,q}^{m,n}(\cdot \middle| \begin{matrix} \cdot \\ \cdot \end{matrix})$ represents the Meijer-G function.

2.2. RF-RIS Link Model

The RF-RIS link is assumed to follow Rayleigh distribution, and the random variable (RV) w_i and b_i are assumed to be independently Rayleigh distributed. Thus, following the central limit theorem for large N [24], R defined in Eq. (6) follows Gaussian distribution with $R \sim N(\frac{N\pi}{4}, \frac{N(16-\pi^2)}{16})$. Therefore, the instantaneous SNR of the RF-RIS link is a non-central chi-square RV with one degree of freedom, and its PDF of the SNR γ_{RIS} is defined as [8, 25]:

$$f_{\gamma_2}(\gamma) = \frac{1}{2\eta^2} \left(\frac{\gamma}{\beta}\right)^{-1/4} \exp\left(-\frac{\gamma + \beta}{2\eta^2}\right) I_{-1/2}\left(\frac{\sqrt{\gamma\beta}}{\eta^2}\right) \tag{10}$$

where $\eta^2 = \bar{\gamma}_{RIS}N(16-\pi^2)/16$, $\beta = \bar{\gamma}_{RIS}\pi^2N^2/16$ and $I_n(\cdot)$ denotes the modified Bessel function of first order. In order to obtain a traceable closed-form analytical expression, the modified Bessel function is thus converted to Meijer-G function by using the identity defined in [26] as:

$$I_{-1/2}\left(\frac{\sqrt{\gamma_2\beta}}{\eta^2}\right) = \pi\sqrt{2}\beta^{-1/4}\gamma^{-1/4}G_{1,3}^{1,0}\left(\frac{\beta}{4\eta^4}\gamma\middle|\begin{matrix}1/2\\0,\,1/2,\,1/2\end{matrix}\right) \tag{11}$$

Then, the RIS link PDF of the SNR γ_{RIS} can be obtained by substituting Eq. (11) into Eq. (10) as follows:

$$f_{\gamma_{RIS}}(\gamma) = \frac{\pi\sqrt{2}}{2\eta}\exp\left(-\frac{\beta}{2\eta^2}\right)\exp\left(-\frac{\gamma}{2\eta^2}\right)\gamma^{-1/8}G_{1,3}^{1,0}\left(\frac{\beta}{4\eta^4}\gamma\middle|\begin{matrix}1/2\\0,\,1/2,\,1/2\end{matrix}\right) \tag{12}$$

Furthermore, by converting $\exp(-\gamma/2\eta^2)$ into infinite series through the identity detailed in [26, Eq. (1.211(3))], the link PDF of the SNR γ_{RIS} can be finally written as:

$$f_{\gamma_{RIS}}(\gamma) = \frac{\pi\sqrt{2}}{2\eta}\exp\left(-\frac{\beta}{2\eta^2}\right)\sum_{k=0}^{\infty}\frac{(-1)^k}{k!\,(2\eta^2)^k}\gamma^{k-1/8}G_{1,3}^{1,0}\left(\frac{\beta}{4\eta^4}\gamma\middle|\begin{matrix}1/2\\0,\,1/2,\,1/2\end{matrix}\right) \tag{13}$$

The RIS link CDF of the SNR γ_{RIS} can be obtained by integrating Eq. (13) through the use of integral identity stated in [27, Eq. (26)] as:

$$F_{\gamma_{RIS}}(\gamma) = \frac{\pi\sqrt{2}}{2\eta}\exp\left(-\frac{\beta}{2\eta^2}\right)\sum_{k=0}^{\infty}\frac{(-1)^k}{k!\,(2\eta^2)^k}\gamma^{k+7/8}G_{2,4}^{1,1}\left(\frac{\beta}{4\eta^4}\gamma\middle|\begin{matrix}1/2,\ (1/8-k)\\0,(-k-7/8),\,1/2,\,1/2\end{matrix}\right) \tag{14}$$

3. STATISTICAL END-TO-END CLOSED-FORM

3.1. Under the DF Relaying Protocol

When the relay node is considered to be DF relaying scheme, the end-to-end instantaneous SNR can be expressed as [28]:

$$\gamma_{DF} = \min\{\gamma_{PLC}, \gamma_{RIS}\} \tag{15}$$

Based on Eq. (15), the equivalent end-to-end CDF of the system can be defined as:

$$\begin{aligned} F_{eq}^{DF}(\gamma) &= Pr\{\min(\gamma_{PLC}, \gamma_{RIS}) < \gamma\} \\ &\triangleq F_{\gamma_{PLC}}(\gamma) + F_{\gamma_{RIS}}(\gamma) - F_{\gamma_{PLC}}(\gamma)\,F_{\gamma_{RIS}}(\gamma) \end{aligned} \tag{16}$$

where $F_{\gamma_{RIS}}(\gamma)$ and $F_{\gamma_{RIS}}(\gamma)$ respectively represent the CDFs of γ_{PLC} and γ_{RIS}.

By putting Eqs. (9) and (14) into Eq. (16), $F_{eq}^{DF}(\gamma)$ for the system can be expressed as:

$$\begin{aligned} F_{eq}^{DF}(\gamma) &= \left[\frac{(1-P_i)}{\Gamma(m_1)}G_{1,2}^{1,1}\left(\frac{m_1}{\Omega_1}\gamma\middle|\begin{matrix}1\\m_1,\,0\end{matrix}\right) + \frac{P_i}{\Gamma(m_2)}G_{1,2}^{1,1}\left(\frac{m_2}{\Omega_2}\gamma\middle|\begin{matrix}1\\m_2,\,0\end{matrix}\right)\right] \\ &\quad + \frac{\pi\sqrt{2}}{2\xi}\exp\left(-\frac{\rho}{2\xi^2}\right)\sum_{k=0}^{\infty}\frac{(-1)^k}{k!\,(2\xi^2)^k}\gamma^{k+7/8}G_{2,4}^{1,1}\left(\frac{\rho}{4\xi^4}\gamma\middle|\begin{matrix}1/2,\,(1/8-k)\\0,(-k-7/8),\,1/2,\,1/2\end{matrix}\right) \\ &\quad - \left[\frac{\pi\sqrt{2}}{2\xi}\exp\left(-\frac{\rho}{2\xi^2}\right)\sum_{k=0}^{\infty}\frac{(-1)^k}{k!\,(2\xi^2)^k}\gamma^{k+7/8}G_{2,4}^{1,1}\left(\frac{\rho}{4\xi^4}\gamma\middle|\begin{matrix}1/2,\,(1/8-k)\\0,(-k-7/8),\,1/2,\,1/2\end{matrix}\right)\right] \\ &\quad \times \left[\frac{(1-P_i)}{\Gamma(m_1)}G_{1,2}^{1,1}\left(\frac{m_1}{\Omega_1}\gamma\middle|\begin{matrix}1\\m_1,\,0\end{matrix}\right) + \frac{P_i}{\Gamma(m_2)}G_{1,2}^{1,1}\left(\frac{m_2}{\Omega_2}\gamma\middle|\begin{matrix}1\\m_2,\,0\end{matrix}\right)\right] \end{aligned} \tag{17}$$

3.2. Under the AF Relaying Protocol

In the case of AF relaying protocol, the end-to-end instantaneous SNR for the scheme can be written as [4]:

$$\gamma_{AF} = \frac{\gamma_{PLC}\gamma_{RIS}}{\gamma_{RIS}+C} \tag{18}$$

where C represents the constant relative to relay gain.

Based on Eq. (18), the equivalent end-to-end CDF for the concerned system under the AF relaying protocol can be expressed as:

$$F_{eq}^{AF}(\gamma) = \int_0^{\infty} Pr\left\{\frac{\gamma_{PLC}\gamma_{RIS}}{\gamma_{RIS}+C} < \gamma\right\} f_{\gamma_{PLC}}(\gamma)\, d\gamma_{PLC} \tag{19}$$

Following the analysis given in [28], the equivalent end-to-end CDF given in Eq. (19) can further be expressed as:

$$F_{eq}^{AF}(\gamma) = F_{\gamma_{PLC}}(\gamma) + \underbrace{\int_0^{\infty} F_{\gamma_{RIS}}\left(\frac{C_\gamma}{x}\right) f_{\gamma_{PLC}}(x+y)dx}_{\beth_1} \tag{20}$$

The integral part of Eq. (20) can thus be expressed by putting Eqs. (8) and (14) into Eq. (20) as follows:

$$\begin{aligned}
\beth_1 \;=\; & \int_0^{\infty} \frac{\pi\sqrt{2}}{2\eta}\exp\left(-\frac{\beta}{2\eta^2}\right)\sum_{k=0}^{\infty}\frac{(-1)^k}{k!\,(2\eta^2)^k}\left(\frac{C\gamma}{x}\right)^{k+7/8} G_{2,4}^{1,1}\left(\frac{\beta C\gamma}{4\eta^4 x}\middle|\begin{matrix}1/2,\,(1/8-k)\\ 0,(-k-7/8)\,,\,1/2,\,1/2\end{matrix}\right)\\
& \times\left[(1-P_s)\left(\frac{m_1}{\Omega_1}\right)^{m_1}\frac{(x+\gamma)^{m_1-1}}{\Gamma(m_1)}\exp\left(-\frac{m_1}{\Omega_1}(x+\gamma)\right)\right.\\
& \left.+P_s\left(\frac{m_2}{\Omega_2}\right)^{m_2}\frac{(x+\gamma)^{m_2-1}}{\Gamma(m_2)}\exp\left(-\frac{m_2}{\Omega_2}(x+\gamma)\right)\right]dx
\end{aligned} \tag{21}$$

By using binominal expansion for $(x+\gamma)^{m_1-1}$ and $(x+\gamma)^{m_2-1}$ through the identity detailed in [26, Eq. (1.111)], $\beth_1$ can be further expressed as:

$$\begin{aligned}
\beth_1 \;=\; & \frac{\pi\sqrt{2}}{2\eta}\exp\left(-\frac{\beta}{2\eta^2}\right)\sum_{k=0}^{\infty}\frac{(-1)^k\,(C\gamma)^{k+7/8}}{k!\,(2\eta^2)^k}\\
& \times\left[\frac{(1-P_s)}{\Gamma(m_1)}\left(\frac{m_1}{\Omega_1}\right)^{m_1}\sum_{q=0}^{m_1-1}\left(\frac{m_1-1}{q}\right)\gamma^{m_1-q-1}\exp\left(-\frac{m_1}{\Omega_1}\gamma\right)\right]\\
& \times\int_0^{\infty} x^{q-(k+7/8)}\exp\left(-\frac{m_1}{\Omega_1}x\right)G_{2,4}^{1,1}\left(\frac{\beta C\gamma}{4\eta^4 x}\middle|\begin{matrix}1/2,\,(1/8-k)\\ 0,(-k-7/8)\,,\,1/2,\;1/2\end{matrix}\right)\Bigg]dx\\
& +\left[\frac{P_s}{\Gamma(m_2)}\left(\frac{m_2}{\Omega_2}\right)^{m_2}\sum_{q=0}^{m_2-1}\left(\frac{m_2-1}{q}\right)\gamma^{m_2-q-1}\exp\left(-\frac{m_2}{\Omega_2}\gamma\right)\right]\\
& \times\int_0^{\infty} x^{q-(k+7/8)}\exp\left(-\frac{m_2}{\Omega_2}x\right)G_{2,4}^{1,1}\left(\frac{\beta C\gamma}{4\eta^4 x}\middle|\begin{matrix}1/2,\,(1/8-k)\\ 0,(-k-7/8)\,,\,1/2,\,1/2\end{matrix}\right)\Bigg]dx
\end{aligned} \tag{22}$$

By inverting the variable $1/x$ in the Meijer-G function through the identity detailed in [26, Eq. (9.31(2))], Eq. (22) can be solved by utilizing the integral identity defined in [26, Eq. (7.813(1))] as:

$$\begin{aligned}
\beth_1 \;=\; & \frac{\pi\sqrt{2}}{2\eta}\exp\left(-\frac{\beta}{2\eta^2}\right)\frac{(1-P_s)}{\Gamma(m_1)}\sum_{k=0}^{\infty}\sum_{q=0}^{m_1-1}\left(\frac{m_2-1}{q}\right)\frac{(-1)^k\,(C\gamma)^{k+7/8}}{k!\,(2\xi^2)^k}\left(\frac{m_1}{\Omega_1}\gamma\right)^{k+m_1-q-1/8}\\
& \times\exp\left(-\frac{m_1}{\Omega_1}\gamma\right)G_{2,4}^{1,1}\left(\frac{4\Omega_1\eta^4}{\beta C m_1\gamma}\middle|\begin{matrix}(k+7/8-q)\,,1,(k+15/8)\,,\,1/2,\,1/2\\ 1/2,\,(k+7/8)\end{matrix}\right)
\end{aligned}$$

$$+\frac{\pi\sqrt{2}}{2\eta}\exp\left(-\frac{\beta}{2\eta^2}\right)\frac{P_s}{\Gamma(m_2)}\sum_{k=0}^{\infty}\sum_{q=0}^{m_2-1}\binom{m_2-1}{q}\frac{(-1)^k(C\gamma)^{k+7/8}}{k!\,(2\xi^2)^k}\left(\frac{m_2}{\Omega_2}\gamma\right)^{k+m_1-q-1/8}$$
$$\times\exp\left(-\frac{m_2}{\Omega_2}\gamma\right)G_{2,4}^{1,1}\left(\frac{4\Omega_1\eta^4}{\beta C m_2\gamma}\middle|\begin{matrix}(k+7/8-q),1,(k+15/8),\,1/2,\,1/2\\ 1/2,\,(k+7/8)\end{matrix}\right) \tag{23}$$

The AF equivalent CDF can be obtained as:

$$\begin{aligned}F_{\gamma}^{AF}(\gamma) \;=\; &\left[\frac{(1-P_s)}{\Gamma(m_1)}G_{1,2}^{1,1}\left(\frac{m_1}{\Omega_1}\gamma\middle|\begin{matrix}1\\ m_1,\,0\end{matrix}\right)+\frac{P_s}{\Gamma(m_2)}G_{1,2}^{1,1}\left(\frac{m_2}{\Omega_2}\gamma\middle|\begin{matrix}1\\ m_2,\,0\end{matrix}\right)\right]\\
&+\frac{\pi\sqrt{2}}{2\xi}\exp\left(-\frac{\beta}{2\eta^2}\right)\frac{(1-P_s)}{\Gamma(m_1)}\sum_{k=0}^{\infty}\sum_{q=0}^{m_1-1}\binom{m_1-1}{q}\frac{(-1)^k(C\gamma)^{k+7/8}}{k!\,(2\eta^2)^k}\left(\frac{m_1}{\Omega_1}\gamma\right)^{k+m_1-q-1/8}\\
&\times\exp\left(-\frac{m_1}{\Omega_1}\gamma\right)G_{5,2}^{1,2}\left(\frac{4\Omega_1\eta^4}{\beta C m_1\gamma}\middle|\begin{matrix}(k+7/8-q),1,(k+15/8),\,1/2,\,1/2\\ 1/2,\,(k+7/8)\end{matrix}\right)\\
&+\frac{\pi\sqrt{2}}{2\xi}\exp\left(-\frac{\beta}{2\eta^2}\right)\frac{P_s}{\Gamma(m_2)}\sum_{k=0}^{\infty}\sum_{q=0}^{m_2-1}\binom{m_2-1}{q}\frac{(-1)^k(C\gamma)^{k+7/8}}{k!\,(2\eta^2)^k}\left(\frac{m_2}{\Omega_2}\gamma\right)^{k+m_2-q-1/8}\\
&\times\exp\left(-\frac{m_2}{\Omega_2}\gamma\right)G_{5,2}^{1,2}\left(\frac{4\Omega_2\eta^4}{\beta C m_2\gamma}\middle|\begin{matrix}(k+7/8-q),1,(k+15/8),\,1/2,\,1/2\\ 1/2,\,(k+7/8)\end{matrix}\right)\end{aligned} \tag{24}$$

4. PERFORMANCE ANALYSIS

In this paper, outage probability and average bit error rate are the performance metrics considered to evaluate the performance of the concerned system. Also, the asymptotic analysis of each of the system performance indicators is obtained.

4.1. Under the DF Relaying Protocol

4.1.1. Outage Probability for the DF

The system outage probability can be described as the probability of the system end-to-end SNR falls below a preset threshold value γ_{th}. In the case of DF relaying protocol, the outage probability of the concerned system can be obtained as:

$$P_{out}^{DF}(\gamma_{th}) = F_{eq}^{DF}(\gamma_{th}) \tag{25}$$

where $F_{eq}^{DF}(\gamma_{th})$ is the equivalent end-to-end CDF of the concerned system given in Eq. (17).

In order to obtained more useful insight about the system performance, the asymptotic CDF $F_{\gamma_{PLC}}(\gamma)$ and $F_{\gamma_{RIS}}(\gamma)$ given in Eqs. (9) and (14) respectively can be obtained by applying the asymptotic series expansion of the Meijer-G function at zero detailed in [11, 26] as follows:

$$F_{\gamma_{PLC}}^{Asy}(\gamma) \approx \frac{(1-P_s)}{\Gamma(m_1+1)}\left(\frac{m_1}{\Omega_1}\gamma\right)^{m_1}+\frac{P_s}{\Gamma(m_2+1)}\left(\frac{m_2}{\Omega_2}\gamma\right)^{m_2} \tag{26}$$

and

$$F_{\gamma_{RIS}}^{Asy}(\gamma) \approx \frac{\pi\sqrt{2}}{2\eta}\exp\left(-\frac{\beta}{2\eta^2}\right)\sum_{k=0}^{\infty}\frac{(-1)^k\gamma^{k+7/8}}{k!\,(2\eta^2)^k\,\Gamma(k+15/8)\,\Gamma(1/8-k)\,\Gamma(1/2)} \tag{27}$$

Asymptotically, the DF outage probability can be expressed as [28, 29]:

$$P_{out,Asy}^{DF}(\gamma_{th}) \approx F_{\gamma_{PLC}}^{Asy}(\gamma_{th}) + F_{\gamma_{RIS}}^{Asy}(\gamma_{th}) \tag{28}$$

By inserting Eqs. (26) and (27) into Eq. (28), the asymptotic outage probability under the DF relaying protocol can be expressed as:

$$P_{out,Asy}^{DF}(\gamma_{th}) \approx \left[\frac{(1-P_s)}{\Gamma(m_1+1)}\left(\frac{m_1}{\Omega_1}\gamma_{th}\right)^{m_1} + \frac{P_s}{\Gamma(m_2+1)}\left(\frac{m_2}{\Omega_2}\gamma_{th}\right)^{m_2}\right] + \frac{\pi\sqrt{2}}{2\eta}\exp\left(-\frac{\beta}{2\eta^2}\right)\sum_{k=0}^{\infty}\frac{(-1)^k\gamma^{k+7/8}}{k!\,(2\eta^2)^k\,\Gamma(k+15/8)\,\Gamma(1/8-k)\,\Gamma(1/2)} \tag{29}$$

4.1.2. Average Bit Error Rate for the DF

The ABER of the system under the DF relay protocol can be defined as [4, 8, 28]:

$$P_b^{DF} = P_e^1 + P_e^2 - 2P_e^1P_e^2 \tag{30}$$

where P_e^1 and P_e^2 are the average error rates of the PLS and RF-RIS link respectively and can be obtained as [28]:

$$P_e = \frac{b^a}{2\Gamma(a)}\int_0^{\infty}\exp(-b\gamma)\,\gamma^{a-1}F_{eq}^i(\gamma)d\gamma, \quad \{i \in DF, AF\} \tag{31}$$

where a and b signify different modulation schemes. In the case of binary phase shift keying (BPSK), $b = 1$ and $a = 1/2$.

Putting Eq. (9) into Eq. (31), the error rate of the PLC link can be expressed as:

$$P_e^1 = \frac{b^a}{2\Gamma(a)}\left[\frac{(1-P_s)}{\Gamma(m_1)}\int_0^{\infty}\exp(-b\gamma)\,\gamma^{a-1}G_{1,2}^{1,1}\left(\frac{m_1}{\Omega_1}\gamma\middle|\begin{matrix}1\\ m_1,\,0\end{matrix}\right)d\gamma + \frac{P_s}{\Gamma(m_2)}\int_0^{\infty}\exp(-b\gamma)\,\gamma^{a-1}G_{1,2}^{1,1}\left(\frac{m_2}{\Omega_2}\gamma\middle|\begin{matrix}1\\ m_2,\,0\end{matrix}\right)d\gamma\right] \tag{32}$$

By utilizing the integral identity defined in [26, Eq. (7.813(1))], the error of the PLC link can be obtained as:

$$P_e^1 = \frac{1}{2\Gamma(a)}\left[\frac{(1-P_s)}{\Gamma(m_1)}G_{2,2}^{1,2}\left(\frac{m_1}{b\Omega_1}\middle|\begin{matrix}1-a,\,1\\ m_1,\,0\end{matrix}\right) + \frac{P_s}{\Gamma(m_2)}G_{2,2}^{1,2}\left(\frac{m_2}{b\Omega_2}\middle|\begin{matrix}1-a,\,1\\ m_2,\,0\end{matrix}\right)\right] \tag{33}$$

Moreover, P_e^2 can be obtained by putting Eq. (14) into Eq. (31) as follows:

$$P_e^2 = \frac{\pi\sqrt{2}}{4\eta\Gamma(a)}\exp\left(-\frac{\beta}{2\eta^2}\right) \sum_{k=0}^{\infty}\frac{(-1)^k}{k!\,(2\eta^2)^k}\int_0^{\infty}\gamma^{k+a+7/8-1}\exp(-b\gamma)\,G_{2,4}^{1,1}\left(\frac{\beta}{4\eta^4}\gamma\middle|\begin{matrix}1/2,\,(1/8-k)\\ 0,(-k-7/8),\,1/2,\,1/2\end{matrix}\right)d\gamma \tag{34}$$

By utilizing the integral identity defined in [26, Eq. (7.813(1))], P_e^2 can be obtained as:

$$P_e^2 = \frac{\pi\sqrt{2}}{4\xi\Gamma(a)}\exp\left(-\frac{\rho}{2\xi^2}\right) \sum_{k=0}^{\infty}\frac{(-1)^k\,b^{-(k+7/8)}}{k!\,(2\xi^2)^k}G_{3,4}^{1,1}\left(\frac{\rho}{4b\xi^4}\middle|\begin{matrix}1-(k+a+7/8),1/2,\,(1/8-k)\\ 0,(-k-7/8),\,1/2,\,1/2\end{matrix}\right) \tag{35}$$

Thus, the overall ABER of the system under DF relaying protocol can be obtained by substituting Eqs. (33) and (35) into Eq. (30).

The asymptotic ABER of the system under the DF relaying protocol can be expressed as:

$$P_b^{Asy} \approx P_e^{1,Asy} + P_e^{2,Asy} \tag{36}$$

where $P_e^{1,Asy}$ and $P_e^{2,Asy}$ are the asymptotic error rates of the PLS and RF-RIS link, respectively.

To determine $P_e^{1,Asy}$, Eq. (26) is substituted into Eq. (31) as follows:

$$P_e^{1,Asy} = \frac{b^a}{2\Gamma(a)}\left[\frac{(1-P_s)}{\Gamma(m_1+1)}\left(\frac{m_1}{\Omega_1}\right)^{m_1}\int_0^\infty \gamma^{m_2+a-1}\exp(-b\gamma)d\gamma + \frac{P_s}{\Gamma(m_2+1)}\left(\frac{m_2}{\Omega_2}\right)^{m_2}\int_0^\infty \gamma^{m_2+a-1}\exp(-b\gamma)d\gamma\right] \tag{37}$$

By applying the integral identity detailed in [26, Eq. (3.326(2))], $P_e^{1,Asy}$ can be expressed as:

$$P_e^{1,Asy} = \frac{1}{2\Gamma(a)}\left[\frac{(1-P_s)\Gamma(m_1+a)b^{-m_1}}{\Gamma(m_1+1)}\left(\frac{m_1}{\Omega_1}\right)^{m_1} + \frac{P_s\Gamma(m_2+a)b^{-m_2}}{\Gamma(m_2+1)}\left(\frac{m_2}{\Omega_2}\right)^{m_2}\right] \tag{38}$$

Also, putting Eq. (27) into Eq. (31), $P_e^{2,Asy}$ can be expressed as:

$$P_e^{2,Asy} = \frac{\pi\sqrt{2}b^b}{4\eta\Gamma(a)}\exp\left(-\frac{\beta}{2\xi^2}\right)\sum_{k=0}^{\infty}\frac{(-1)^k}{k!\,(2\eta^2)^k\,\Gamma(k+15/8)\,\Gamma(1/8-k)\,\Gamma(1/2)} \times \int_0^\infty \gamma^{k+7/8+a-1}\exp(-b\gamma)d\gamma \tag{39}$$

By using the integral identity detailed in [26, Eq. (3.326(2))], Eq. (39) can be expressed as:

$$P_e^{2,Asy} = \frac{\pi\sqrt{2}}{4\eta\Gamma(a)}\exp\left(-\frac{\beta}{2\eta^2}\right)\sum_{k=0}^{\infty}\frac{(-1)^k\Gamma(k+a+7/8)\,b^{-(k+7/8)}}{k!\,(2\eta^2)^k\,\Gamma(k+15/8)\,\Gamma(1/8-k)\,\Gamma(1/2)} \tag{40}$$

Thus, the asymptotic ABER of the system under DF can be obtained by putting Eqs. (38) and (40) into Eq. (36) as follows:

$$P_b^{Asy} \approx \frac{1}{2\Gamma(a)}\left[\frac{(1-P_i)\Gamma(m_1+a)b^{-m_1}}{\Gamma(m_1+1)}\left(\frac{m_1}{\Omega_1}\right)^{m_1} + \frac{P_i\Gamma(m_2+a)b^{-m_2}}{\Gamma(m_2+1)}\left(\frac{m_2}{\Omega_2}\right)^{m_2} + \frac{\pi\sqrt{2}}{2\eta}\exp\left(-\frac{\beta}{2\eta^2}\right)\sum_{k=0}^{\infty}\frac{(-1)^k\Gamma(k+a+7/8)\,b^{-(k+a+7/8)}}{k!\,(2\eta^2)^k\,\Gamma(k+15/8)\,\Gamma(1/8-k)\,\Gamma(1/2)}\right] \tag{41}$$

4.2. Under AF Relaying Protocol

4.2.1. Outage Probability for the AF

In the case of AF relaying protocol, the end-to-end outage probability can be defined as [4]:

$$P_{out}^{AF}(\gamma_{th}) = Pr\{\gamma < \gamma_{th}\} = F_{eq}^{AF}(\gamma_{th}) \tag{42}$$

where $F_{eq}^{AF}(\gamma_{th})$ is the equivalent end-to-end CDF of the concerned system detailed in Eq. (24).

4.3. Average Bit Error Rate for the AF

The ABER of the system under the AF relaying protocol for different modulation schemes can be obtained by putting Eq. (24) into Eq. (31), and the ABER is expressed as:

$$P_b^{AF} = \frac{b^a}{2\Gamma(a)}\left[P_b^1 + P_b^2 + P_b^3\right] \tag{43}$$

where the first term can be expressed as:

$$P_b^1 = \frac{(1-P_s)}{\Gamma(m_1)} \int_0^\infty \exp(-b\gamma)\,\gamma^{a-1} G_{1,2}^{1,1}\left(\frac{m_1}{\Omega_1}\gamma \middle| \begin{matrix} 1 \\ m_1,\, 0 \end{matrix}\right) d\gamma + \frac{P_s}{\Gamma(m_2)} \int_0^\infty \exp(-b\gamma)\,\gamma^{a-1} G_{1,2}^{1,1}\left(\frac{m_2}{\Omega_2}\gamma \middle| \begin{matrix} 1 \\ m_2,\, 0 \end{matrix}\right) d\gamma \quad (44)$$

By applying the integral identity detailed in [26, Eq. (7.813(1))], Eq. (44) can be obtained as:

$$P_b^1 = \frac{(1-P_s)}{\Gamma(m_1)} b^{-a} G_{2,2}^{1,2}\left(\frac{m_1}{b\Omega_1}\middle| \begin{matrix} 1-a,\, 1 \\ m_1,\, 0 \end{matrix}\right) + \frac{P_s}{\Gamma(m_2)} b^{-a} G_{2,2}^{1,2}\left(\frac{m_2}{b\Omega_2}\middle| \begin{matrix} 1-a,\, 1 \\ m_2,\, 0 \end{matrix}\right) \quad (45)$$

The second term of Eq. (43) can be expressed as:

$$P_b^2 = \frac{\pi\sqrt{2}}{2\eta}\exp\left(-\frac{\beta}{2\xi^2}\right)\frac{(1-P_s)}{\Gamma(m_1)}\sum_{k=0}^{\infty}\sum_{q=0}^{m_1-1}\binom{m_2-1}{q}\frac{(-1)^k (C\gamma)^{k+7/8}}{k!\,(2\eta^2)^k}\left(\frac{m_1}{\Omega_1}\gamma\right)^{k+m_1-q-1/8}\int_0^\infty \gamma^{k+m_1-q-a-9/8} \times \exp\left(\left(-\frac{m_1}{\Omega_1}+b\right)\gamma\right) G_{2,4}^{1,1}\left(\frac{4\Omega_1\eta^4}{\beta C m_1\gamma}\middle| \begin{matrix} (k+7/8-q),\,1,\,(k+15/8),\,1/2,\,1/2 \\ 1/2,\,(k+7/8) \end{matrix}\right) d\gamma \quad (46)$$

By utilizing the identity in [26], the Meijer-G function is inverted, and Eq. (46) can be further expressed as:

$$P_b^2 = \frac{\pi\sqrt{2}}{2\eta}\exp\left(-\frac{\beta}{2\eta^2}\right)\frac{(1-P_s)}{\Gamma(m_1)}\sum_{k=0}^{\infty}\sum_{q=0}^{m_1-1}\binom{m_2-1}{q}\frac{(-1)^k (C\gamma)^{k+7/8}}{k!\,(2\eta^2)^k}\left(\frac{m_1}{\Omega_1}\right)^{k+m_1-q-1/8}\int_0^\infty \gamma^{k+m_1-q-a-9/8} \times \exp\left(\left(-\frac{m_1}{\Omega_1}+b\right)\gamma\right) G_{2,5}^{2,1}\left(\frac{\beta C m_1\gamma}{4\Omega_1\eta^4}\middle| \begin{matrix} 1/2,\,(1/8+k) \\ (q-k+1/8),\,0,\,(-k-7/8),\,1/2,\,1/2 \end{matrix}\right) d\gamma \quad (47)$$

Through the integral identity defined in [26, Eq. (7.813(1))], Eq. (47) can be obtained as:

$$P_b^2 = \frac{\pi\sqrt{2}}{2\eta}\exp\left(-\frac{\beta}{2\eta^2}\right)\frac{(1-P_s)}{\Gamma(m_1)}\sum_{k=0}^{\infty}\sum_{q=0}^{m_1-1}\binom{m_2-1}{q}\frac{(-1)^k (C\gamma)^{k+7/8}}{k!\,(2\eta^2)^k}\left(\frac{m_1}{\Omega_1}\right)^{k+m_1-q-1/8} \left(-\frac{m_1}{\Omega_1}+b\right)^{q-k-m_1-a+1/8} G_{3,5}^{1,3}\left(\frac{\beta C m_1}{4\eta^4(m_1+b\Omega_1)}\middle| \begin{matrix} (q-k-m_1-a+9/8),\,1/2,\,(1/8-k) \\ (q-k+1/8),\,0,\,(-k-7/8),\,1/2,\,1/2 \end{matrix}\right) \quad (48)$$

Following the same approach as in the case of P_b^2, the last term of Eq. (43) can be expressed as:

$$P_b^3 = \frac{\pi\sqrt{2}}{2\eta}\exp\left(-\frac{\beta}{2\eta^2}\right)\frac{P_s}{\Gamma(m_2)}\sum_{k=0}^{\infty}\sum_{q=0}^{m_2-1}\binom{m_2-1}{q}\frac{(-1)^k (C\gamma)^{k+7/8}}{k!\,(2\eta^2)^k}\left(\frac{m_2}{\Omega_2}\gamma\right)^{k+m_2-q-1/8} \left(-\frac{m_2}{\Omega_2}+b\right)^{q-k-m_2-a+1/8} G_{3,5}^{1,3}\left(\frac{\beta C m_2}{4\eta^4(m_2+b\Omega_2)}\middle| \begin{matrix} (q-k-m_2-a+9/8),\,1/2,\,(1/8-k) \\ (q-k+1/8),\,0,\,(-k-7/8),\,1/2,\,1/2 \end{matrix}\right) \quad (49)$$

5. NUMERICAL RESULTS AND DISCUSSIONS

In this section, the numerical results on the derived analytical expression of the system outage probability and average error rate with asymptotic expressions are presented under the DF and AF relaying schemes. The results indicate the analytical results perfectly matched with the Montel-Carlo simulations under the same system conditions which proved the correctness of analytical results. Except otherwise stated, the system parameters are set to: $m_1 = m_2 = 4$, $\gamma_{th} = 5\,dB$, $C = 1.2$, $P_s = 0.8$, and $\bar{\gamma}_{PLC} = \bar{\gamma}_{RIS} = \bar{\gamma}$.

In Figure 2, the impact of number of reflecting elements on the system performance under the DF relaying protocol is illustrated. The results show that the use of RIS significantly improves the

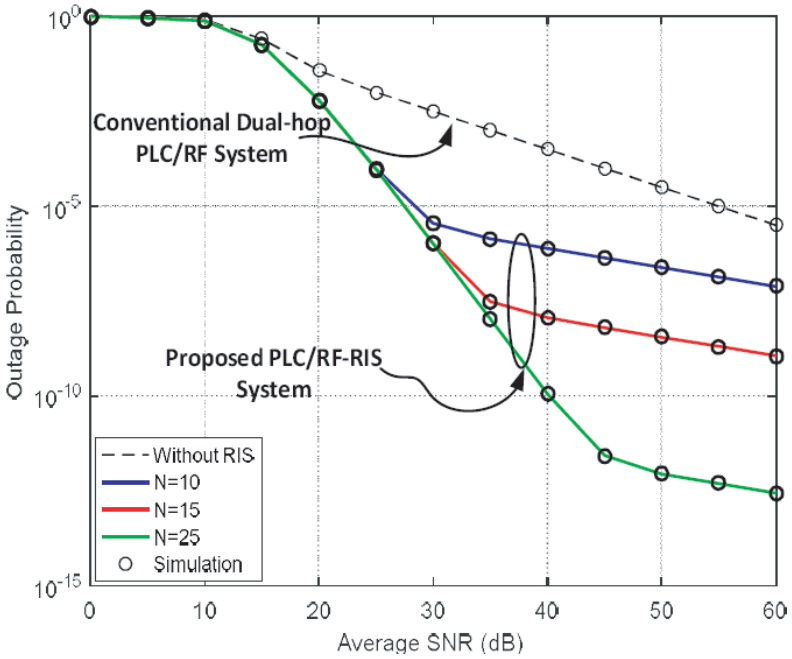

Figure 2. Outage performance of the system under DF relaying protocol for different values for N.

system performance compared to conventional non-RIS system. It can also be deduced that the system performance improves with the increase in the number of reflecting elements.

The outage probability performances of the system for different values of threshold SNR γ_{th} under both relaying protocols are depicted in Figure 3. The results show that the decrease in the values of threshold SNR γ_{th} deteriorates the system outage performance. It can be observed that the AF relaying protocol outperforms the DF relaying protocol under the same system condition.

Moreover, the effect of P_s on the system outage probability is presented in Figure 4. The results

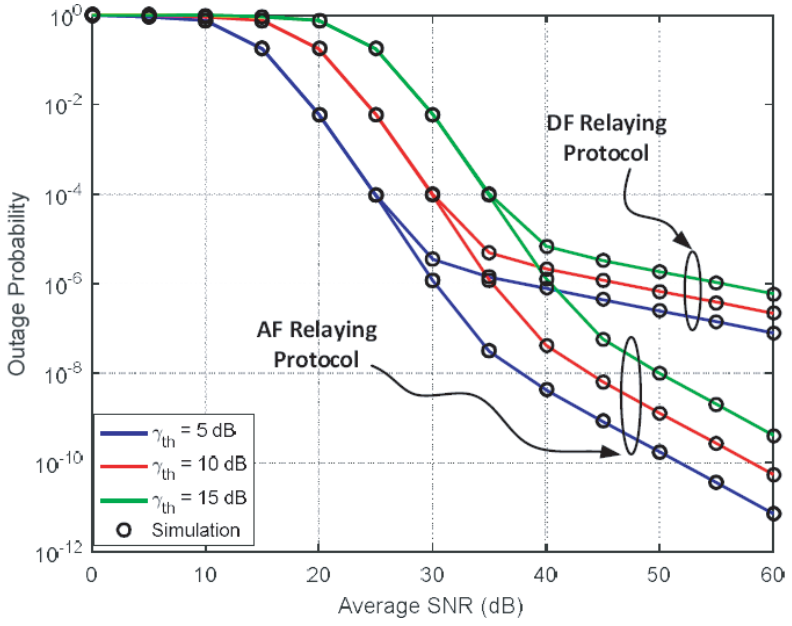

Figure 3. Outage performance of the system under the DF and AF relaying protocols for different values of threshold SNR γ_{th} at $N = 10$.

depict that the increase in P_s significantly degrades the system performance; a lower value of P_s indicates a weak effect of impulsive noise on the PLC link, and the high value of P_s signifies a strong effect of impulsive noise of the concerned system. In addition, it can be clearly observed that the asymptotic results perfectly match the analytical results at high SNR regime. This justifies the tightness of the derived asymptotic expression.

In Figure 5, the impact of number of reflecting elements on the system error rate for both DF and

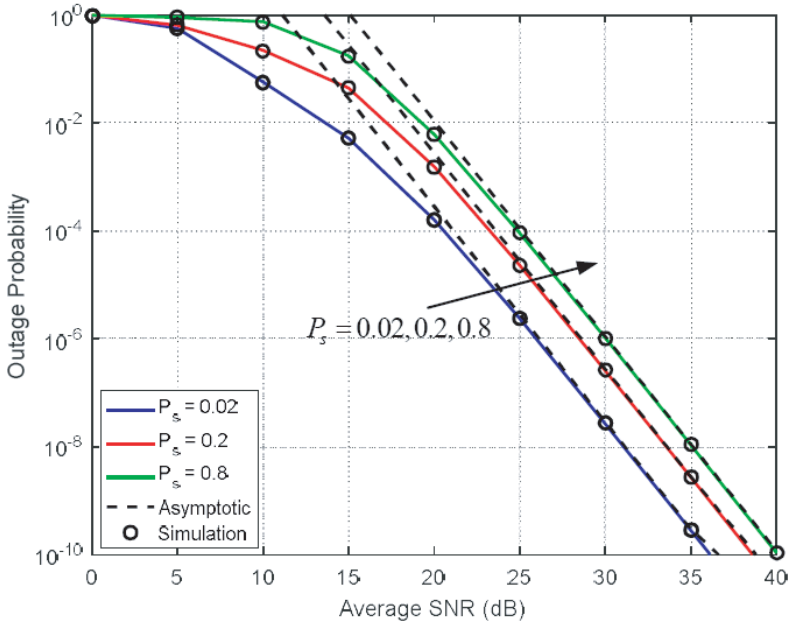

Figure 4. Impact of P_s on the system outage probability performance under the DF relaying protocol at $N = 30$.

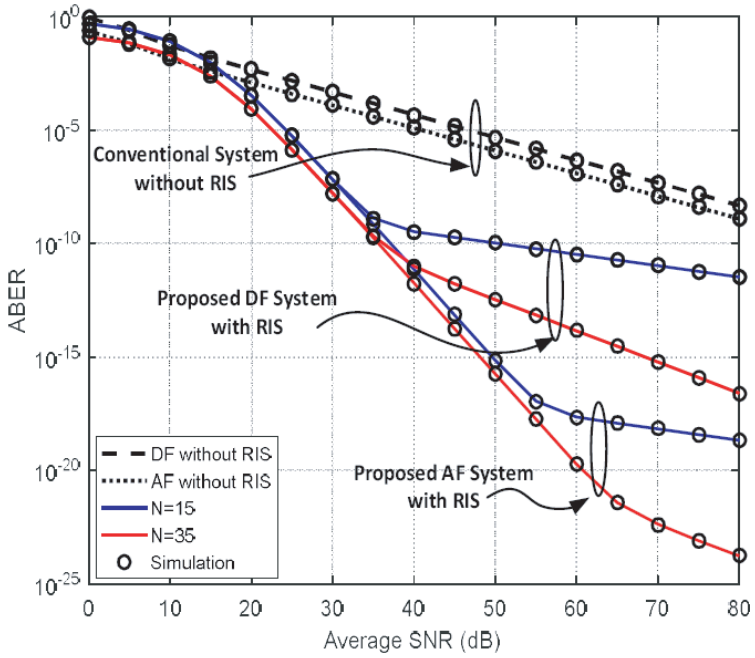

Figure 5. Effect of number of reflecting elements N on the system error rate under the DF and AF relaying protocol.

AF relaying schemes is provided. It can be clearly observed that the use of RIS significantly improves the system error rate compared to non-RIS system for both relaying schemes. The results also show that there is improvement in the system error rate with increase in the number of reflecting elements, and AF relaying scheme offers better performance of the system than DF.

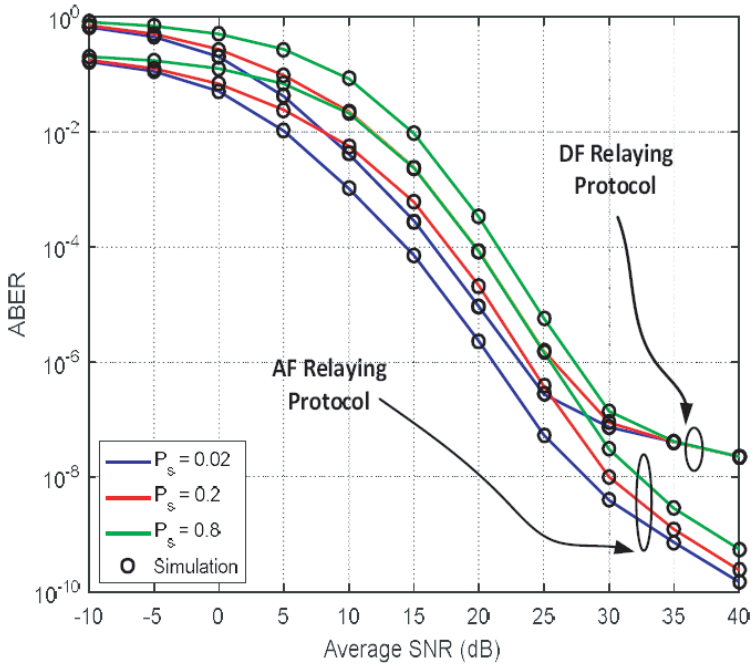

Figure 6. Error rate performance of the system for different values of P_s under the DF and AF relaying protocol.

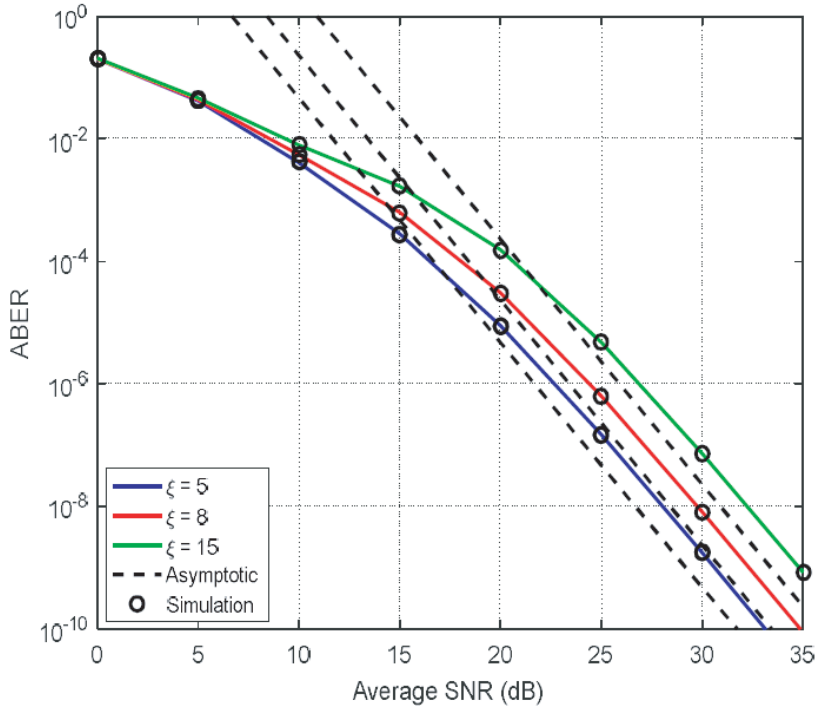

Figure 7. Impact of ξ of the system error rate under the DF relaying scheme.

The system error rate performances for different values of P_s under the AF and DF relaying protocols are demonstrated in Figure 6. The results depict that the increase in P_s significantly degrades the system performance with a lower value of P_s indicates weak effect of impulsive noise on the PLC link. It can also be observed from the results that for any given value of P_s, the AF relaying protocol offers the system better performance than the DF relaying protocol.

Furthermore, the system average BERs for different values of ξ under the DF relaying protocol are depicted in Figure 7. The results indicate that the increase in ξ leads to decrease in the system average error rate. The results also indicate convergence between the asymptotic results and analytical results at high SNR regime.

6. CONCLUSION

The performance analysis of a dual-hop RIS-aided PLC system under the DF and AF relaying schemes is presented in this study. The analytical closed-form expressions of the outage probability and average error rate of the system are derived. To gain more performance insight about the derived analytical expressions, the asymptotic expressions are obtained for the performance metrics at high SNR. It is illustrated by the results that the analytical results match perfectly with the Montel-Carlo simulations which validate the accuracy of the derived closed-form expressions. In addition, the results indicate that the number of reflecting elements in RIS significantly improves the system performance compared with the conventional dual-hop PLC systems. It can also be deduced that the impulsive noise affects the overall performance of the concerned system.

REFERENCES

1. Gheth, W., K. M. Rabie, B. Adebisi, M. Ijaz, and G. Harris, "Performance analysis of integrated power-line/visible-light communication systems with AF relaying," *2018 IEEE Global Communications Conference (GLOBECOM)*, 1–6, IEEE, 2018.
2. Rabie, K. M., B. Adebisi, H. Gacanin, and S. Yarkan, "Energy-per-bit performance analysis of relay-assisted power line communication systems," *IEEE Transactions on Green Communications Networking*, Vol. 2, No. 2, 360–368, 2018.
3. Gheth, W., K. M. Rabie, B. Adebisi, M. Ijaz, G. Harris, and A. Alfitouri, "Hybrid power-line/wireless communication systems for indoor applications," *2018 11th International Symposium on Communication Systems, Networks & Digital Signal Processing (CSNDSP)*, 1–6, IEEE, 2018.
4. Yang, L., X. Yan, S. Li, D. B. da Costa, and M.-S. Alouini, "Performance analysis of dual-hop mixed PLC/RF communication systems," *arXiv preprint arXiv:.09051*, 2020.
5. Anastasiadou, D. and T. Antonakopoulos, "Multipath characterization of indoor power-line networks," *IEEE Transactions on Power Delivery*, Vol. 20, No. 1, 90–99, 2005.
6. Rozman, M., A. Ikpehai, B. Adebisi, and K. M. Rabie, "Channel characterisation of cooperative relaying power line communication systems," *2016 10th International Symposium on Communication Systems, Networks and Digital Signal Processing (CSNDSP)*, 1–5, IEEE, 2016.
7. Makarfi, A. U., R. Kharel, K. M. Rabie, O. Kaiwartya, X. Li, and D.-T. Do, "Reconfigurable intelligent surfaces based cognitive radio networks," *arXiv preprint arXiv:.10946*, 2020.
8. Odeyemi, K. O., P. A. Owolawi, and O. O. Olakanmi, "Performance analysis of reconfigurable intelligent surface assisted underwater optical communication system," *Progress In Electromagnetics Research*, Vol. 98, 101–111, 2020.
9. Yang, L., Y. Yang, D. B. da Costa, and I. Trigui, "Performance analysis of an interference-limited RIS-aided network," *arXiv preprint arXiv:.07479*, 2020.
10. Tang, Z., T. Hou, Y. Liu, J. Zhang, and L. Hanzo, "Physical layer security of intelligent reflective surface aided NOMA networks," *arXiv preprint arXiv:.03417*, 2020.
11. Odeyemi, K. O., P. A. Owolawi, and O. O. Olakanmi, "Reconfigurable intelligent surface assisted mobile network with randomly moving user over Fisher-Snedecor fading channel," *Physical Communication*, Vol. 43, 101186, 2020.

12. Basar, E., M. Di Renzo, J. De Rosny, M. Debbah, M.-S. Alouini, and R. Zhang, "Wireless communications through reconfigurable intelligent surfaces," *IEEE Access*, Vol. 7, 116753–116773, 2019.
13. Basar, E., "Transmission through large intelligent surfaces: A new frontier in wireless communications," *2019 European Conference on Networks and Communications (EuCNC)*, 112–117, IEEE, 2019.
14. Dubey, A. and R. K. Mallik, "PLC system performance with AF relaying," *IEEE Transactions on Communications*, Vol. 63, No. 6, 2337–2345, 2015.
15. Ahiadormey, R. K., P. Anokye, H.-S. Jo, and K.-J. Lee, "Performance analysis of two-way relaying in cooperative power line communications," *IEEE Access*, Vol. 7, 97264–97280, 2019.
16. Passerini, F. and A. M. Tonello, "Analog full-duplex amplify-and-forward relay for power line communication networks," *IEEE Communications Letters*, Vol. 23, No. 4, 676–679, 2019.
17. Salem, A., K. M. Rabie, K. A. Hamdi, E. Alsusa, and A. M. Tonello, "Physical layer security of cooperative relaying power-line communication systems," *2016 International Symposium on Power Line Communications and Its Applications (ISPLC)*, 185–189, IEEE, 2016.
18. Yang, L., W. Guo, and I. S. Ansari, "Mixed dual-hop FSO-RF communication systems through reconfigurable intelligent surface," *IEEE Communications Letters*, Vol. 24, No. 7, 1558–1562, 2020.
19. Yang, L., W. Guo, D. B. da Costa, and M.-S. Alouini, "Free-space optical communication with reconfigurable intelligent surfaces," *arXiv preprint arXiv:.00547*, 2020.
20. Yang, L., F. Meng, J. Zhang, M. O. Hasna, and M. Di Renzo, "On the performance of RIS-assisted dual-hop UAV communication systems," *IEEE Transactions on Vehicular Technology*, Vol. 69, No. 9, 10385–10390, 2020.
21. Jani, M., P. Garg, and A. Gupta, "Performance analysis of a mixed cooperative PLC-VLC system for indoor communication systems," *IEEE Systems Journal*, Vol. 14, No. 1, 469–476, 2019.
22. Jani, M., P. Gargt, and A. Gupta, "Modeling and outage analysis of DF relay assisted mixed PLC-VLC system," *2018 Twenty Fourth National Conference on Communications (NCC)*, 1–5, IEEE, 2018.
23. Prudnikov, A., Y. A. Brychkov, and O. Marichev, *Integrals and series Volume 3: More Special Functions*, Taylor and Francis, Oxford, UK, 2003.
24. Proakis, J. G. and M. J. I. Salehi, *Digital Communications*, McGraw-Hill, New York, 1995.
25. Yang, L. and Y. Yuan, "Secrecy outage probability analysis for RIS-assisted NOMA systems," *Electronics Letters*, Vol. 56, No. 23, 1254–1256, 2020.
26. Gradshteyn, I. S. and I. M. Ryzhik, *Table of Integrals, Series, and Products*, Academic Press, 2014.
27. Adamchik, V. and O. Marichev, "The algorithm for calculating integrals of hypergeometric type functions and its realization in REDUCE system," *Proceedings of the International Symposium on Symbolic and Algebraic Computation*, 212–224, 1990.
28. Li, S., L. Yang, and D. B. da Costa, "Performance analysis of UAV-based mixed RF-UWOC transmission systems," *arXiv preprint arXiv:.09062*, 2020.
29. Yang, L., M.-S. Alouini, and I. S. Ansari, "Asymptotic performance analysis of two-way relaying FSO networks with nonzero boresight pointing errors over double-generalized gamma fading channels," *IEEE Transactions on Vehicular Technology*, Vol. 67, No. 8, 7800–7805, 2018.